Vol. 102, No. 3; March 2013

NATIONALPARK-FORSCHUNG
IN DER SCHWEIZ
(Switzerland Research Park Journal)

Active Control of Structures and Reliability Analysis by Subset Simulation Method

H. Shariatmadar1, G. Behnam Rad2

1Associated Professor, Dept. of Civil Engineering, Ferdowsi University of Mashhad

2PhD student, Dept. of Civil Engineering, Ferdowsi University of Mashhad

Abstract: Uncertainty is inherent in the control of all engineering structures. This uncertainty can arise from control hardware malfunctions, neglected system dynamics and other inadequacies of the mathematical model, errors in identifying parameters, model reduction, degradation of the structure over time, etc. If the uncertainties are not properly considered in the design of a control strategy, the performance of the controlled structure may be severely degraded, and an otherwise stable nominal structure may even become unstable due to actuator control forces. While the modeling assumptions have become more elaborate and accurate over the years, the reliability analysis of stochastic structural systems still remains a challenging problem. Therefore the reliability analysis of uncertain structural systems subjected to dynamic loads is of great engineering interest and poses a challenging computational problem. Because of the uncertainty inherent in engineering structures, consistent probabilistic stability/performance measures are essential to accurately assessing and comparing the robustness of structural control systems. Several reliability estimation methods, procedures and algorithms with various capabilities, accuracy and efficiency have been suggested in the past. A quantitative comparison of these approaches is considered to be most instrumental and useful for the engineering community. In this article, a simulation approach, called “Subset Simulation”, is used to compute small failure probabilities encountered in reliability analysis of engineering systems. In part I, several illustrative examples are presented to demonstrate the efficiency of the used simulation and compare its results to those of other methods. In part II, several examples of SDOF and MDOF seismically excited structures with active protective systems are applied to compare their results to each other. The results of two part show that “Subset Simulation” method is robust and efficient in estimating the probability of failure of structural systems with complex failure regions, large numbers of random variables, and small probabilities of failure.

Keywords: Reliability analysis; Subset simulation; Active structural control; Failure probability

1-Introduction

Advanced construction methods and durable construction materials are insufficient for an important structure when it exposes with extreme external impacts. In order to minimize these huge impacts, control strategies are widely used in high rise and large structures. Control methods become more popular with the help of development at technology and computers. Huge dynamic impacts can be result of earthquakes, huge storms, explosions and other external forces. Earthquake factor is the most important one because of its inherent uncertainty and international importance.

Uncertainty is inherent in the control of all engineering structures. This uncertainty can arise from control hardware malfunctions, neglected system dynamics and other inadequacies of the mathematical model, errors in identifying parameters, model reduction, degradation of the structure over time, etc. If the uncertainties are not properly considered in the design of a control strategy, the performance of the controlled structure may be severely degraded, and an otherwise stable nominal structure may even become unstable due to actuator control forces.

While the modeling assumptions have become more elaborate and accurate over the years, the reliability analysis of stochastic structural systems still remains a challenging problem.

The reliability analysis of uncertain structural systems subjected to random loads is of great engineering interest and poses a challenging computational problem. The probability of failure can be expressed as

$$P_f = P\{G(\theta) \le 0\} = \int_{G(\theta)} f(\theta)d\theta = \int I_F(\theta) f(\theta)d\theta \qquad (1)$$

where the vector $\theta = [\theta_1, \dots, \theta_n]$ represents an uncertain state of the system with joint probability function $f(\theta)$. $G(\theta)$ is the failure or limit state function, defining a safe state when G > 0 and a failure state when G < 0. The hyper-surface separating the safe from the failure domains G = 0 is called the limit state. F is the failure region. I_F is an indicator function; where $I_F(\theta) = 1$ if $\theta \in F$ and $I_F(\theta) = 0$ otherwise.

A large number of reliability analysis methods have been developed during the last three decades. The most commonly used methods include first order reliability method (FORM) or second order reliability method (SORM), as well as improved simulation approaches such as the many variants of advanced Monte Carlo methods. These methods suffer from a number of well known limitations. For example, although FORM and SORM are often very efficient, they both require the availability of an explicit formulation of the failure function and they are designed to determine the most likely design point and do not necessarily give very accurate estimates of the probability of failure.

Also, neither method is robust when solving complex limit state equations, such as highly non-linear failure equations or a combination of failure functions [1, 2].

The Monte Carlo simulation (MCS) method has been widely used in the past because of its robustness and its ability to solve problems with complex failure regions [3, 4]. Its main disadvantage stems from its inefficiency when solving problems with large numbers of random variables and small probabilities (e.g.,$P_F \le 10^{-3}$), because the number of samples, and hence the number of system analyses required to achieve a given accuracy, is proportional to $1/P_F$. Essentially, finding small probabilities requires information from rare samples corresponding to failure, and on average it will require many samples before a failure occurs. Despite the prodigious development in computer technology, direct Monte Carlo simulation, which is the most generally applicable procedure, is inefficient or infeasible in engineering practice, due to, for example:

• The complexity in the behavior of structural systems of practical interest. This often requires the numerical solution of nonlinear equations with multiple unknowns, which imposes a heavy computational burden even in deterministic setting.
• The high number of random parameters that must be incorporated in order to accurately account for the uncertainties observed.
• The complexity in the probabilistic characteristics of certain random parameters (i.e. non-stationary, non-Gaussianity, etc.).
It is emphasized that the excursion probabilities computed are relatively low, which implies that direct Monte Carlo is practically not applicable for such problems, because it would require unacceptably high numbers of simulations.
Recent efforts to improve the ability to analyze the reliability of real scale structural problems have led to the implementation of Markov Chain simulation algorithms [5–9]. In particular, Au and Beck [8] have developed a new Markov Chain-based advanced simulation method known as the subset simulation which was found to be efficient and is able to handle structural dynamic systems with large numbers of random variables and small probabilities of failure.
In this approach, the failure probability is expressed as a product of conditional probabilities of some chosen intermediate failure events, the evaluation of which only requires simulation of more frequent events. The problem of evaluating a small failure probability in the original probability space is thus replaced by a sequence of simulations of more frequent events in the conditional probability spaces. The conditional probabilities, however, cannot be evaluated efficiently by common techniques, and therefore a Markov Chain Monte Carlo simulation (MCMCS) method based on Metropolis algorithm [10] is used.

2. Review of subset simulation

When the probability of failure is estimated by means of simulation, the difficulty often increases with decreasing failure probability. Basically, the smaller the P_f, the more rare failure event is, and the more the number of samples required realizing failure events for computing P_f.
The basic concept behind the subset simulation approach developed by Au and Beck [8] centers on the fact that a small probability of failure can be expressed as a product of large values of conditional failure probabilities by introducing several intermediate failure events. This would convert a rare event into a sequence of more frequent ones. During the simulation, conditional samples are generated from specially designed Markov Chains so that they gradually populate each intermediate failure region until they cover the whole failure domain.
Let F denote the failure domain. The subset failure regions Fi are arranged such that $F_1 \ni F_2 \ni \ldots \ni F_m = F$ to form a decreasing sequence of failure events. The probability of failure P_f can be represented as the probability of falling in the final subset F_m given that on the previous step, the event belonged to subset F_{m-1}. This can be represented by the equation

$$P_f = P(F_m|F_{m-1})P(F_{m-1}) \quad (2)$$

By recursively repeating the process Eq. (3) is obtained.

$$P_f = P(F_m|F_{m-1})P(F_{m-1}) = P(F_1)\prod_{i=2}^{m} P(F_i|F_{i-1}) \quad (3)$$

Eq. (3) shows that instead of calculating P_f directly, P_f can be calculated as the product of several conditional probabilities. With a proper choice of the conditional events, the

conditional failure probabilities can be made sufficiently large so that they can be estimated using a small number of samples. If the failure domain F of a system is defined as the exceedance of the demand B over a given capacity b, that is $F = (B > b)$, then the intermediate failure regions can be represented as

$$F_i = (B_i > b_i) \quad (4)$$

The probability of failure can be rewritten as

$$P_f = P(B > b) = P(B > b_1) \prod_{i=2}^{m} P(B > b_i | B > b_{i-1}) \quad (5)$$

where $0 < b_1 < b_2 < \ldots < b_m = b$ form an increasing sequence of intermediate threshold values.

Because it is difficult to know a priori what optimum intermediate threshold values to choose in order to get reasonable estimates of the conditional probabilities, the intermediate thresholds, b_i, are chosen ''adaptively'' so that the conditional probabilities are approximately equal to a common specified value, p_0. Experience shows that $p_0 = 0.1$ is a prudent choice [8].

To compute P_f based on Eq. (3), one needs to compute the probabilities $P(F_1)$, and $P(F_i|F_{i-1})$. The unconditional probability $P(F_1)$ for the first subset can be readily estimated by Monte Carlo simulation (MCS). It is also possible to compute the conditional failure probabilities using MCS. This will necessitate verifying that each generated sample θ belongs to F_{i-1} before even checking whether θ belongs to F_i or not. Samples that do not satisfy F_{i-1} must be rejected which creates large inefficiencies.

To overcome the problem associated with generating samples that satisfy the conditional probability, a Markov Chain Monte Carlo simulation technique based on the M–H (Metropolis–Hastings) Algorithm [11,12] has been proposed by Au and Beck [8]. The M–H algorithm is based on the Markov Chain simulation approach using Eq. (5). Accordingly, the approach requires generating a new sample ε given that a previously generated sample θ already belongs to F_{i-1}. To execute the move, a proposal probability density function $q(\theta, \varepsilon)$ must be selected. The proposal distribution governs the choice of the candidate samples and consequently the efficiency of the M–H algorithm. Approaches for selecting $q(\theta, \varepsilon)$ will be presented further below. Given $q(\theta, \varepsilon)$, the procedure consists of the following steps:

1. Start with a given a current $\tilde{\theta}_{i-1} = \left[\tilde{\theta}_{i-1}^{(1)}, \ldots, \tilde{\theta}_{i-1}^{(n)}\right]$ (n being the number of random variables) that belongs to the subset region F_{i-1}.
2. For each random variable, generate a pre-candidate component $\varepsilon_i^{(j)}$ from the proposal probability density function (PDF) $q_j\left(0 \middle| \theta_{i-1}^{(j)}\right)$ (j = 1, . . . , n).
3. Compute the move probability $\alpha(\theta, \varepsilon)$ also known as the acceptance probability:

$$\alpha_i^{(j)} = \pi_j\left(\varepsilon_i^{(j)}\right) q_j\left(\theta_{i-1}^{(j)} \middle| \varepsilon_i^{(j)}\right) / \pi_j\left(\theta_{i-1}^{(j)}\right) q_j\left(\varepsilon_i^{(j)} \middle| \theta_{i-1}^{(j)}\right) \quad (6)$$

where π is the target stationary distribution.

4. Set the jth component of $\tilde{\theta}_i^{(j)}$ according to

$$\tilde{\theta}_i^{(j)} = \begin{cases} \varepsilon_i^{(j)} \text{ with probability } \min(1, \alpha_i^{(j)}) \\ \theta_{i-1}^{(j)} \text{ with probability } 1 - \min(1, \alpha_i^{(j)}) \end{cases} \quad (7)$$

5. Generate an independent random variable, u, from the uniform probability distribution $U(0, 1)$. If $u \leq \alpha_j$, the move is accepted and if $u > \alpha_j$, the move is not allowed.

6. Accept the candidate $\tilde{\theta}_i^{(j)}$ if it belongs to F_{i-1}; otherwise reject it and take the current state as the new sample so that $\theta_i^{(j)} = \theta_{i-1}^{(j)}$.

The procedure for adaptively generating samples of θ conditional on $F_i\ (i = 1, \ldots, m)$ is summarized as follows.

1. Generate N sample vectors $(\theta_{0,k}: k = 1, \ldots, N)$ by direct Monte Carlo simulation such that they are independent identical distribution (iid) from the proposal PDF q. The subscript '0' here denotes that the samples belong to ''conditional level 0'' or the ''unconditional'' case.
2. Use $(\theta_{0,k}: k = 1, \ldots, N)$to obtain the N responses $(B_{0,k}: k = 1, \ldots, N)$ for each vector θ_0.
3. The value of b_1 is chosen such that $[(1 - p_0)N]$ responses lie outside the subset F_1 and $p_0 N$ samples belong to $F_1 = (B > b_1)$.
4. The $p_0 N$ samples among the original $(\theta_{0,k}: k = 1, \ldots, N)$ that lie within F_1 are the conditional samples at 'conditional level 1'.
5. Starting from each of the samples that belong to F_1, the M–H algorithm is used to simulate an additional $[(1 - p_0)N]$ conditional samples so that there are a total of N conditional samples at conditional level 1.
6. The value of b_2 is then chosen such that the responses of $[(1 - p_0)N]$ samples of those generated in step 5 lie outside $F_2 = (B > b_2)$. Note that the sample estimate for $P(F_2|F_1) = P(B > b_2|B > b_1)$ is automatically equal to p_0.
7. Again, there will be $p_0 N$ samples within F_2. These samples are conditional on F_2 and provide 'seeds' for applying the M–H algorithm to simulate an additional $[(1 - p_0)N]$ conditional samples so that there is a total of N conditional samples at conditional level 2.
8. The procedure is repeated for higher conditional levels until the samples at conditional level $(m - 1)$ have been generated.

The approach used for generating the samples for the subset simulation method is schematically illustrated in Fig.1. Fig.1a shows the unconditional N samples generated at level 0 and the corresponding probability distribution curve of the response B. Fig.1b illustrates how failure region F_1 is defined to contain $p_0 N$ samples, where p_0 is a preset conditional probability. Fig.1c shows how the $p_0 N$ samples are augmented by generating additional samples to obtain a total of N samples in F_1. Fig.1d shows how F_2 is subdivided from F_1 such that $p_0 N$ samples are included in F_2. The process of regenerating new samples in F_2 and dividing F_2 into new subsets is continued using the same approach. Note that the proposal PDF affects the generation of the candidate samples given the current samples, and controls the efficiency of the Markov Chain in populating the failure region [8].

3. Numerical examples of part I

Subset simulation described in the previous section is used to estimate the probability of failure for a set of widely used limit state functions (LSF) of various levels of complexity. The following five problems labeled LSF_1 through LSF_5 were collected from the published literature and are solved using the MCMCS algorithm. The results are compared with those obtained using the classical Monte Carlo simulation and the traditional FORM algorithm. The examples were generally selected for analysis by the various authors who proposed them because of their overall complexities which render them difficult to solve using traditional FORM/SORM algorithms. These complexities are due to the presence of multiple design

points, highly nonlinear failure equations, the presence of saddle points, or their concave shape [11].

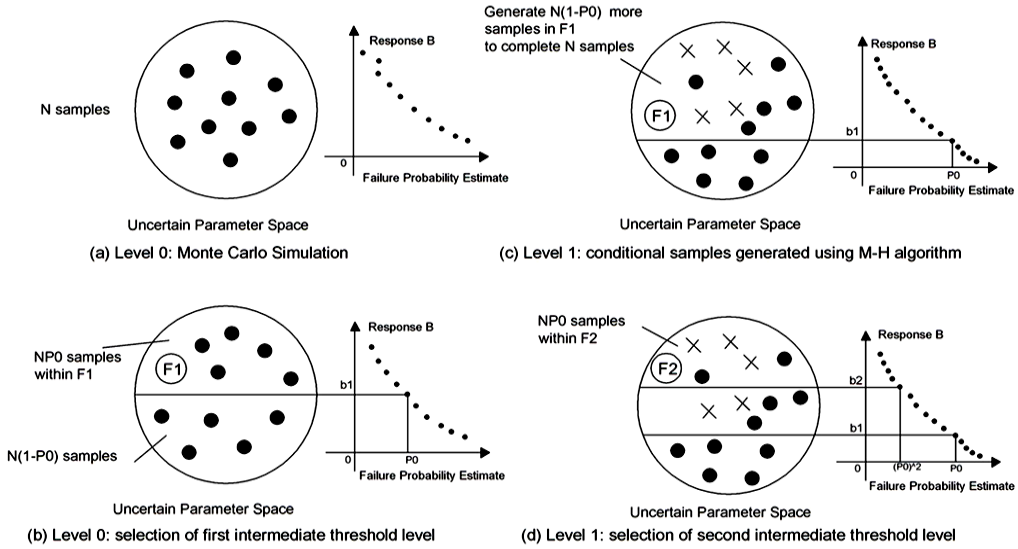

Fig.1. Illustration of subset simulation procedure [11].

3.1. $\mathbf{LSF_1}$ – Noisy limit state function with six random variables [12]

The noisy equation is given as a function of six Normal random variables X_1 through X_6:

$$LSF_1 = X_1 + 2X_2 + 2X_3 + X_4 - 5X_5 - 5X_6 + .001\sum_{i=1}^{6}\sin(100\,X_i) \quad (8)$$

$$X_1 = X_2 = X_3 = X_4 \sim LN(120,12)$$

$$X_5 \sim LN(50,15), \qquad X_6 \sim LN(40,12)$$

3.2. $\mathbf{LSF_2}$ – Multiple failure points with two random variables [12]

In this case, the limit state function is a hyperbola and has two design points which makes it difficult to solve using the FORM algorithm.

$$LSF_2 = X_1X_2 - PL \quad (9)$$

P and L are deterministic parameters with

$$P = 14.614;\ L = 10.0$$

While X_1 and X_2 are normal random variables.

$$X_1 \sim N(78064.4, 11709.7)$$

$$X_2 \sim N(0.0104, 1.56 * 10^{-3})$$

3.3. $\mathbf{LSF_3}$ – Concave LSF [13]

This limit state function is represented by the equation

$$LSF_3 = -0.5(X_1 - X_2)^2 - \frac{(X_1+X_2)}{\sqrt{2}} + 3 \quad (10)$$

$$X_1 = X_2 \sim N(0,1)$$

3.4. $\mathbf{LSF_4}$ – Nonlinear LSF with saddle point [14]

The presence of the saddle point complicates the identification of the design point.

$$\mathrm{LSF}_4 = 2 - \mathrm{X}_2 - 0.1\mathrm{X}_1^2 + 0.06\mathrm{X}_1^3 \quad (11)$$

$$\mathrm{X}_1 = \mathrm{X}_2 \sim \mathrm{N}(0,1)$$

3.5. $\mathbf{LSF_5}$ – Fourth order limit state function [15]

This highly nonlinear equation is given as:

$$\mathrm{LSF}_5 = 3 - \mathrm{X}_2 + (4\mathrm{X}_1)^4 \quad (12)$$

$$\mathrm{X}_1 = \mathrm{X}_2 \sim \mathrm{N}(0,1)$$

Table 1 provides a summary of the several reliability estimation methods results using the probabilistic analysis software FERUM [16].

Table 1

Results of reliability estimation methods for five limit states with the same number of samples.

LSF NO.	No. of samples at each conditional level	Total samples	MCMC Pf	MCS Pf	FORM Pf	Accurate Pf
1	1500	3000	1.24E-02	1.22E-02	_	1.22E-02
2	4500	31500	1.39E-07	_	_	1.48E-07
3	1500	3000	1.05E-01	1.06E-01	1.36E-03	1.05E-01
4	1500	3000	3.47E-02	3.51E-02	2.28E-02	3.47E-02
5	2000	8000	1.71E-04	_	1.35E-03	1.80E-04

The results summarized in Table 1 demonstrate the efficiency of the subset simulation (Markov Chain Monte Carlo simulation technique based on the Metropolis–Hastings Algorithm (MCMCS)), that was capable of providing very good accuracy for the probability of failure up to the order of 10^{-7}. The values listed in Table 1 are the average values based on 50 independent runs. The results show that the First Order Reliability method (FORM), in LSF_1 and LSF_2 cannot provide probability of failure, because of existence more design points and for other cases results have not good accuracy. Also Monte Carlo Simulation method (MCS), in LSF_2 and LSF_5 is not efficient because of problem has large numbers of random variables and small probabilities of failure. Therefore the results indicate that MCMCS technique is very useful in problems with various levels of complexity.

4. Control system

Advanced design methods and even high performance construction materials are insufficient for special structure when it is subjected to extreme dynamic excitation loads. In order to optimize the performance of structure, control strategies are widely used. Control methods become more popular with the help of development at technology and computers. Structural control strategies have two main type and these are passive and active systems. Also hybrid and semi-active systems are used in buildings.

Mitigation of the structural response, under seismic action, can be achieved bringing suitable changes to the mechanical parameters of the system, in particular to the terms of the stiffness and damping matrices. To obtain the optimal solution for this problem, it is often necessary to calibrate the coefficients of the motion equation in measure incompatible with

the properties of the common structural materials. This can be carried out by active control techniques. The entity of the action produced by the actuators is regulated by a control (closed) loop, based on an algorithm which, as in the present essay, is assumed as a linear function of the response parameters.
As a matter of fact, during its 30 years of history, the active control numbers many examples both of linear control and of non-linear control for linear structures, based on the idea of a quadratic performance index.
In this study, active tendon control was virtually analyzed on two different model buildings. One of these models was a single degree of freedom system (SDOF) which was experimentally examined before by Chung, Reinhorn and Soong [17]. The other system was a three storey multiple degree of freedom system (MDOF) which was also experimentally examined by Chung, Lin, Reinhorn and Soong [18].
Active tendon control systems consist of four pre-stressed cables, two actuators and a control element. In order to control more than one degree, additional four pre-stressed cables, two actuators and a controller is also needed for each degree. While half of the cables and actuators exist on one side of the building, the others exist on the opposite side.

5. Problem formulation

In the equations of motion for the structure, the existence of uncertainty is assumed which can be modeled by a q-dimensional vector of random parameters Δ, with a given mean μ_Δ, covariance σ_Δ, and joint probability distribution $F_\Delta(\delta)$. The state space representation of the equations of motion for an n-degree-of-freedom structure is given by

$$\dot{z} = A(\Delta)z + B(\Delta)u + E(\Delta)w \tag{13}$$

with measurement equation

$$y = C(\Delta)z + D(\Delta)u + F(\Delta)v \tag{14}$$

where the vector z is a 2n-dimensional state vector of displacements and velocities, A is a $2n \times 2n$ matrix composed of the parameters of the structure (masses, stiffnesses, damping values, etc.), u is an r-dimensional vector of control forces, B is a $2n \times 2n$ matrix specifying the points of application of the control forces, w is an l-dimensional excitation vector, E is a $2n \times l$ matrix specifying the manner in which the excitation affects the structure, y is an m-dimensional measurement vector, C is an $m \times 2n$ matrix through which combinations of the states are measured, D is an $m \times r$ matrix specifying the feed-through terms in the measurement, F is an $m \times m$ matrix indicating how the measurement noise affects the measurement, and v is an m-dimensional measurement noise vector. The vector $[w'\ v']'$ is assumed to be a white noise with mean and joint autocorrelation given by

$$E\begin{bmatrix} w \\ v \end{bmatrix} = 0 \tag{15}$$

$$E\left[\begin{Bmatrix} w(t) \\ v(t) \end{Bmatrix}\{w'(t+\tau)\ v'(t+\tau)\}\right] = 2\pi S\delta(\tau) \tag{16}$$

where $E[.]$ is the expected value operator, S is a constant two-sided spectral density matrix, and $\delta(.)$ is the Dirac delta function. Nonwhite noises can be incorporated into the problem formulation by augmenting the equations of motion with appropriate disturbance shaping filters [19].
For a broad class of control strategies, the closed-loop state space description can be written as

$$\dot{\tilde{z}} = A_{cl}(\Delta)\tilde{z} + E_{cl}\begin{Bmatrix} W \\ V \end{Bmatrix} \quad (17)$$

where $\tilde{z}$ is the state vector ($\tilde{z}$ may also contain states of the controller or the disturbance shaping filter), $A_{cl}(\Delta)$ is the closed-loop state matrix, and E_{cl} is the matrix indicating how the disturbance and measurement noise affect the dynamics of the closed-loop system. For example, if we assume that the structure state variables are perfectly measurable and that state feedback control is employed, i.e., $u = -Kz$ then $\tilde{z} = z$ and the closed-loop state space matrix is given by

$$A_{cl}(\Delta) = A(\Delta) - B(\Delta)K \quad (18)$$

where K is the control gain matrix.

5.1. Objective performance measures

For stochastically excited structures, a tractable measure of performance robustness can be given in terms of the RMS structural responses. For example, if one is concerned with the Root Mean Square (RMS) responses σ_z exceeding specified threshold levels σ_{0_i}, then a series of performance limit-state functions can be defined as

$$g_i^P[\Delta;\, u, t] = \sigma_{0_i} - \sigma_{z_i}[\Delta;\, u, t] \quad (19)$$

Here, the notation $\sigma_{z_i}[\Delta;\, u, t]$ is chosen to emphasize the fact that the RMS response is a time varying function depending on both the parametric uncertainty Δ and the chosen control strategy $u(\theta)$, $0 \le \theta \le t$. The performance limit-state probability P_f is defined as

$$P_f = \max_{0 \le t \le t_f} P\left\{\bigcup_{i=1}^{v} g_i^P[\Delta;\, u, t] \le 0\right\} \quad (20)$$

where t_f is some time larger than the duration of the disturbance, and v is the number of critical responses. Thus, P_f represents the probability of exceedance of one or more of the target RMS structural responses.

A further problem simplification can be made by concentrating on the stationary response. For many problems of interest, the RMS structural responses take maximum values when they achieve stationary [19]. Under this assumption, Eq. (20) reduces to

$$P_f = P\left\{\bigcup_{i=1}^{v} g_i^P(\Delta;\, u) \le 0\right\} \quad (21)$$

where $g_i^P(\Delta;\, u) = \sigma_{0_i} - \sigma_{z_i}[\Delta;\, u]$, and $\sigma_{z_i}[\Delta;\, u]$ represents the ith stationary RMS displacement response. In terms of the probability density function $f_\Delta(\delta)$, the performance limit-state probability can be written as

$$P_f = \int_{\bigcup_{j=1}^{v} \sigma_{z_i}[\Delta;\, u] \ge \sigma_{0_i}} \int f_\Delta(\delta)\, d(\delta) \quad (22)$$

This can be viewed as a reliability problem for a series of components $g_i^P(\Delta;\, u)$. To evaluate this expression, First Order Reliability Method (FORM), Monte Carlo Simulation (MCS) and Subset Simulation (Markov Chain Monte Carlo simulation technique based on the Metropolis–Hastings Algorithm (MCMCS)) can be employed.

For the linear dynamical system in Eq. (17), the RMS responses, or equivalently the response covariance matrix $\sum_{\tilde{z}} = E[\tilde{z}\tilde{z}']$, are obtained as the solution of the Lyapunov equation,

$$\dot{\sum}_{\tilde{z}} = A_{cl} \sum_{\tilde{z}} + \sum_{\tilde{z}} A_{cl}' + 2\pi E_{cl} S E_{cl}' \quad (23)$$

with the initial condition $\sum_{\tilde{z}}(0) = \sum_0$ [20]. The stationary covariance matrix can be obtained by solving Eq. (23) with $\dot{\sum}_{\tilde{z}} = 0$.

6. Numerical examples of part II

The probabilistic robustness measures will be illustrated using two examples of seismically excited structures. The first example deals with the single degree-of-freedom (SDOF) tendon controlled structure reported by Chung et al. [17]. A more complex structure, a three degree-of-freedom (3DOF), single-bay building with tendon controller, is examined in the second example. This structure is similar to that reported in [18]. Because the maximum non-stationary RMS response is often well represented by the stationary responses [19], the examples will focus on the robustness measures based on the stationary responses.

6.1. Single degree-of-freedom structure

Model of the SDOF system with active tendons and changes of tendon forces are shown in Fig. 2. Horizontal displacement of the system is x and $\ddot{x}_g$ is the ground acceleration. R is the pre-stress force of each tendon during static state. In dynamic state, while one of the crosswise tendons is being tensed by tensile force, the other one is being unloaded because of compressive force. Absolute value of control force must be smaller than pre-stress force because tendons cannot carry compressive force.

Equation of motion for uncontrolled building is shown in Eq. (24). Equation (25) is for the SDOF system with active tendons. Horizontal control force is $-k_c u\cos\alpha$ for each tendon.

$$m\ddot{x} + c\dot{x} + kx = -m\ddot{x}_g \tag{24}$$

$$m\ddot{x} + c\dot{x} + kx = -m\ddot{x}_g - 4k_c u\cos\alpha \tag{25}$$

where x is the displacement of the first floor mass with respect to the ground, u is the position of the hydraulic actuator, k is the stiffness and c is the damping of the walls of the structure, m is the mass of the floor, and $\ddot{x}_g$, is the ground acceleration. Control is obtained by positioning the cylinder at the base of the structure, thereby stretching one set of active tendons and releasing the second set of active tendons to induce forces into the structure.

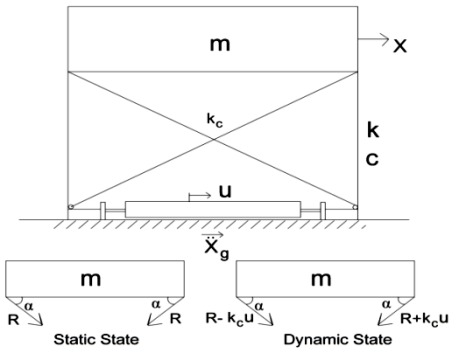

Fig.2. Model of SDOF system with active tendons and control forces [21].

The state space representation of the equations of motion is then

$$\dot{z} = \begin{bmatrix} 0 & 1 \\ \frac{-k}{m} & \frac{-c}{m} \end{bmatrix} z + \begin{bmatrix} 0 \\ \frac{-4k_c\cos\alpha}{m} \end{bmatrix} u + \begin{bmatrix} 0 \\ -1 \end{bmatrix} \ddot{x}_g \tag{26}$$

where $z = [x\ \dot{x}]'$.

The controller is obtained by assuming that the ground acceleration can be modeled as a Gaussian white noise and minimizing the quadratic performance index given by

$$J = \lim_{T\to\infty} \frac{1}{T} E\left[\int_0^T (kx^2 + \gamma k_c u^2)dt\right] \tag{27}$$

where γ is a control design parameter, as γ increase, more weight is placed on the input energy, as γ decrease, more weight is placed on the strain energy and as γ is infinitive, corresponds to the uncontrolled case. The probabilistic robustness measures are examined for the control strategy that neglects the system time delay and minimizes the performance index given in Eq. (27) to obtain a constant gain, state feedback controller. This control strategy is denoted the Linear Quadratic Regulator (LQR) controller.
In what follows, we assume that the controllers are known and deterministic. The mass m, stiffness k and damping c are assumed to have mean values equal to their nominal values and to have a coefficient of variation of 10%. For simplicity the variants are assumed to be statistically independent Gaussian variants. Table 2 provides a summary of the problem parameters.

Table 2
Model parameters for the single degree-of-freedom structure [22]

	Mean(μ)	Standard deviation(σ)
$\mathrm{m(lb-s^2/in)}$	16.69	1.669
$\mathrm{c(lb-s/in)}$	9.02 ($\xi = 1.24\%$)	0.902
$\mathrm{k(lb/in)}$	7934	793.4
$\mathrm{k_c(lb/in)}$	2124	0.0
$\mathrm{\alpha(degrees)}$	36	0.0

For the LQR controller, we have chosen $\gamma = 1, \gamma = 100, \gamma = 2000$ for the performance index in Eq. (27). The problem of finding $\mathrm{k_1}$ and $\mathrm{k_2}$ is a standard one in optimal control theory by solving the Riccati matrix equation. The three control gain matrices are given in Table 3.

Table 3
Transfer functions for LQR controllers used in the examples

	$\mathrm{k_1}$	$\mathrm{k_2}$
$\gamma = 1$	-1.0969	-0.07169
$\gamma = 100$	-0.01607	-0.00762
$\gamma = 2000$	-0.00081	-0.00107

The nominal RMS displacement and velocity responses σ_x, $\sigma_{\dot{x}}$ the RMS control action σ_u, and the performance index J for the nominal structure subjected to a unit intensity white noise are given in Table 4. Note that the smallest performance index is obtained by the $\gamma = 1$.
Table 5 provides a summary of the several reliability estimation methods results using the probabilistic analysis software FERUM [16].

Table 4
Summary of RMS responses for the nominal structure subject to a unit intensity white noise excitation

LQR control	$\sigma_x(\text{in})$	$\sigma_{\dot{x}}(\text{in/s})$	$\sigma_u(\text{in})$	$J(\text{in}-\text{lbs})$
$\gamma = 1$	0.0162	.4934	.0531	8.071
$\gamma = 100$	.0642	1.4107	.0118	62.28
$\gamma = 2000$	.1254	2.7343	0.003	162.99

Table 5

Summary of reliability estimation methods results for the SDOF structure

CASE_ONE			P_f	β
$\gamma = 1$	σ_0 =0 .018(in)	MCMC	1.96E-02	2.065
		MCS	1.23E-01	1.16
		FORM	1.45E-01	1.06
$\gamma = 100$	σ_0 = 0.087(in)	MCMC	2.95E-04	3.44
		MCS	3.32E-03	2.71
		FORM	3.07E-03	2.74
$\gamma = 2000$	σ_0 = 0.17(in)	MCMC	3.48E-04	3.40
		MCS	3.42E-03	2.7
		FORM	3.86E-03	2.66

Results show that subset simulation method (Markov Chain Monte Carlo simulation technique based on the Metropolis–Hastings Algorithm (MCMCS)), has reached to smaller probabilities of failure (P_f) and larger reliability index (β) than the other methods.

Fig. 3 shows that in large failure probabilities, all of the three methods provide close failure probabilities, but with decreasing the failure probability, MCS and FORM methods are coincided until $P_f \geq 10^{-3}$ and then MCS method can not provides smaller failure probability, on the other hand, MCMCS method can calculates failure probabilities until 10^{-7}, so this method is very usefull in active controlled structures.

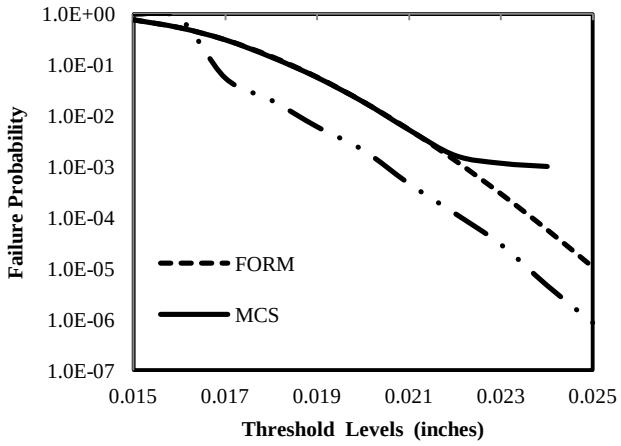

Fig. 3. Estimation for the probability of failure for different threshold levels (σ_0).

In terms of the performance robustness, Fig. 4 provides the cumulative probability distribution function for the RMS displacement response obtained via MCS. As shown here, use of smaller control design parameter (γ), more weight is placed on the strain energy and small RMS displacement responses obtain than the other, therefore use of active control system can reduce the RMS displacement responses and failure probability.

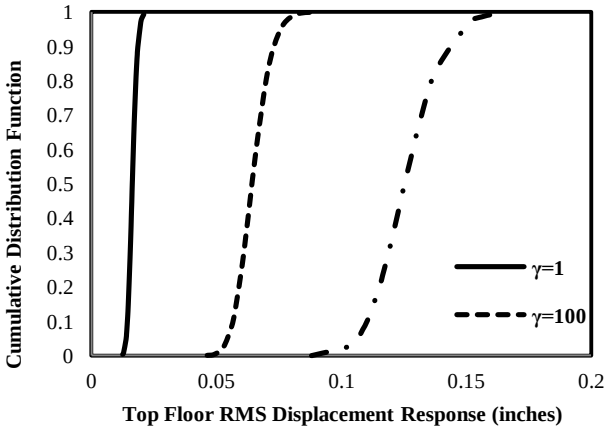

Fig. 4. Cumulative probability distribution functions of RMS displacement response.

6.2. Three degree-of-freedom structure

Now a more complex structures, a three-story, single-bay building subjected to a one-dimensional earthquake excitation $\ddot{x}_g$, with tendon controller is used. In Fig. 5 three cases of the tendon placement are shown. In case A, tendons exist only in first storey. Tendons exist in all floors in case B and C, but in case C, all actuators are placed on the ground floor. If pre-stress forces at the tendons are R, the tendon forces during dynamic state are shown in Fig. 6. Assuming a simple shear frame model for the building, the mass, stiffness and damping matrices are presented in Eq. (28). The equations of motion were given in space state form, Eq. (29) is for case A, Eq. (30) is for case B and Eq. (31) is for case C.

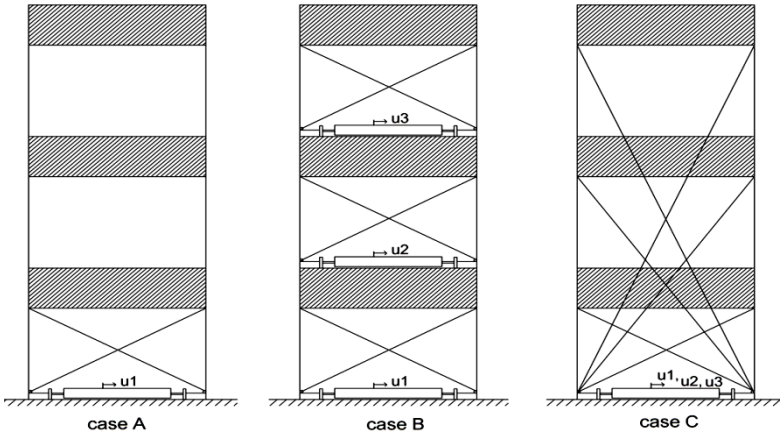

Fig. 5. Model of MDOF system with active tendons for three cases [23].

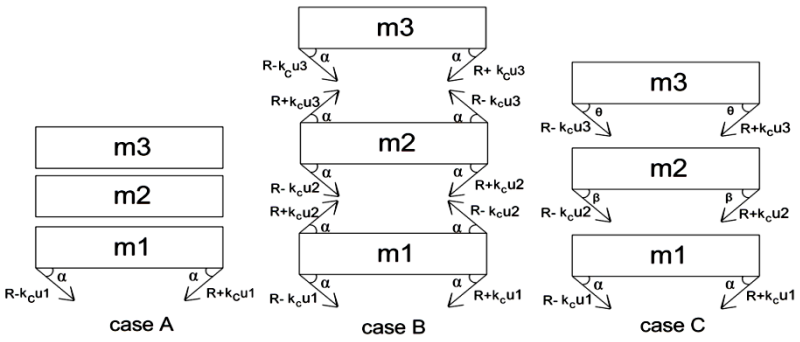

Fig. 6. Tendon forces at dynamic state for all cases [21].

$$[M]=\begin{bmatrix} m_1 & 0 & 0 \\ 0 & m_2 & 0 \\ 0 & 0 & m_3 \end{bmatrix},[C]=\begin{bmatrix} c_1+c_2 & -c_2 & 0 \\ -c_2 & c_2+c_3 & -c_3 \\ 0 & -c_3 & c_3 \end{bmatrix},[K]=\begin{bmatrix} k_1+k_2 & -k_2 & 0 \\ -k_2 & k_2+k_3 & -k_3 \\ 0 & -k_3 & k_3 \end{bmatrix} \quad (28)$$

$$[M]\ddot{X}+[C]\dot{X}+[K]X=-[M][1]\ddot{x}_g-4k_c\cos\alpha\begin{bmatrix} u_1 \\ 0 \\ 0 \end{bmatrix} \quad (29)$$

$$[M]\ddot{X}+[C]\dot{X}+[K]X=-[M][1]\ddot{x}_g+4k_c\cos\alpha\begin{bmatrix} -1 & 1 & 0 \\ 0 & -1 & 1 \\ 0 & 0 & -1 \end{bmatrix}\begin{bmatrix} u_1 \\ u_2 \\ u_3 \end{bmatrix} \quad (30)$$

$$[M]\ddot{X}+[C]\dot{X}+[K]X=-[M][1]\ddot{x}_g-4k_c\cos\alpha\begin{bmatrix} u_1\cos\alpha \\ u_2\cos\beta \\ u_3\cos\theta \end{bmatrix} \quad (31)$$

where m_i, c_i, k_i, are the mass, damping and stiffness, respectively, associated with the ith floor of the building, and u is the position of the hydraulic actuator. Equations (29-31) can be written in matrix form as

$$M_s\ddot{x}+C_s\dot{x}+K_sx=B_su-M_s\Gamma_s\ddot{x}_g \quad (32)$$

Defining the state vector of the system as $z=[x',\dot{x}']'$, the state space matrices in Eq. (13) are then

$$A = \begin{bmatrix} 0 & I \\ -M_s^{-1}K_s & -M_s^{-1}C_s \end{bmatrix}, B = \begin{bmatrix} 0 \\ M_s^{-1}B_s \end{bmatrix}, \text{and} E = \begin{bmatrix} 0 \\ -\Gamma_s \end{bmatrix} \quad (33)$$

The controller is assumed to be known and deterministic, and the variables modeling the mass, damping and stiffness are assumed to be Gaussian random variants with a 10% coefficient of variation. Table 6 provides a summary of the model parameters. Note that the nominal parameters were chosen to match closely the characteristics of the experimental structure reported by Chung et al. [18], in that it has similar modal frequencies and dampings.

As in [18], the controller is obtained by minimizing the quadratic performance index given by

$$J = \lim_{T\to\infty} \frac{1}{T} E\left[\int_0^T (x' k_s x + \gamma k_c u^2) dt\right] \quad (34)$$

For each case, we have chosen three control design parameters. Results are given in Table 7.

Table 6

Model parameters of the three-story structure

	Mean(μ)	Standard deviation(σ)
$m_1(lb - s^2/in)$	5.6	0.56
$m_2(lb - s^2/in)$	5.6	0.56
$m_3(lb - s^2/in)$	5.6	0.56
$c_1(lb - s/in)$	2.6	0.26
$c_2(lb - s/in)$	6.3	0.63
$c_3(lb - s/in)$	0.35	0.035
$k_1(lb/in)$	5034	503.4
$k_2(lb/in)$	10965	1096.5
$k_3(lb/in)$	6135	613.5
$k_c(lb/in)$	2124	0
$\alpha(degrees)$	36	0
$\beta(degrees)$	55	0
$\theta(degrees)$	65	0

Table 7

Transfer functions for LQR controllers used in the examples

		Control gain matrix [K]					
case A	$\gamma = 1$	-0.9658	-0.0063	-0.0002	-0.0394	-0.0397	-0.0397
	$\gamma = 100$	-0.0115	-0.0044	0	-0.0047	-0.0048	-0.0048
	$\gamma = 1500$	-0.0001	-0.001	0	-0.001	-0.001	-0.001
case B	$\gamma = 1$	-	-0.0062	0	-0.0395	-0.0397	-0.0397

		0.9667					
		-0.0255	0.0149	0.0175	-0.0002	-0.0003	-0.0003
		-0.2760	-0.2431	0.5195	0	0	-0.0001
		-0.0105	-0.004	-0.0015	-0.0047	-0.0048	-0.0048
	$\gamma = 100$	-0.0014	0.0006	0.0029	0	0	0
		-0.0167	0.0013	0.0155	0	0	0
		0.0001	-0.0010	0	-0.0010	-0.0010	-0.0010
	$\gamma = 1500$	0.0003	-0.0001	0.0003	0	0	0
		-0.0027	-0.0052	0.0079	0	0	0
	$\gamma = 1$	-1.2530	-0.0110	0.0192	-0.030	-0.0301	-0.0301
case C	$\gamma = 100$	-0.044	-0.026	0.0367	-0.0048	-0.0049	-0.0049
	$\gamma = 1500$	-0.0026	-0.0039	0.0043	-0.0012	-0.0012	-0.0012

Tables 8, 9, 10 provide a summary of the several reliability estimation methods results using the probabilistic analysis software FERUM [16].

Results show that subset simulation method (MCMCS), has reached to suitable and smaller probabilities of failure than other methods while FORM method cannot provides appropriate responses. Figures 7, 8 and 9 show the failure probability estimates for different threshold levels σ_0 for case A, case B and case C, respectively.

Table 8

Summary of reliability estimation methods results for the MDOF structure (case A)

case A			P_f	β
γ=1	σ_0=0.025(in)	MCMC	6.60E-01	0
		MCS	5.15E-01	0
		FORM	5.00E-01	0
γ=100	σ_0=0.12(in)	MCMC	2.42E-02	1.98
		MCS	1.63E-01	0.99
		FORM	4.97E-01	0
γ=1500	σ_0=0.25(in)	MCMC	1.59E-02	2.15
		MCS	1.22E-01	1.16
		FORM	5.00E-01	0

Table 9

Summary of reliability estimation methods results for the MDOF structure (case B)

case B			P_f	β
γ=1	σ_0=0.025(in)	MCMC	9.37E-02	1.32
		MCS	3.82E-01	0.3
		FORM	5.04E-01	0
γ=100	σ_0=0.12(in)	MCMC	2.31E-02	1.99
		MCS	1.66E-01	0.97
		FORM	4.96E-01	0
γ=1500	σ_0=0.25(in)	MCMC	1.59E-02	2.15
		MCS	1.26E-01	1.15
		FORM	5.00E-01	0

Table 10

Summary of reliability estimation methods results for the MDOF structure (case C)

case C			P_f	β
γ=1	σ_0=0.025(in)	MCMC	9.70E-04	3.10
		MCS	1.07E-03	3.07
		FORM	4.99E-01	0
γ=100	σ_0=0.12(in)	MCMC	9.70E-04	3.10
		MCS	0	0
		FORM	4.98E-01	0
γ=1500	σ_0=0.25(in)	MCMC	9.70E-04	3.10
		MCS	1.45E-03	2.98
		FORM	5.00E-01	0

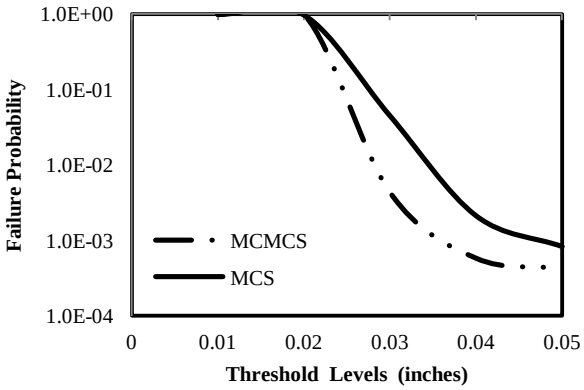

Fig. 7. Estimation for the probability of failure for different threshold levels σ_0 for case A (γ=1).

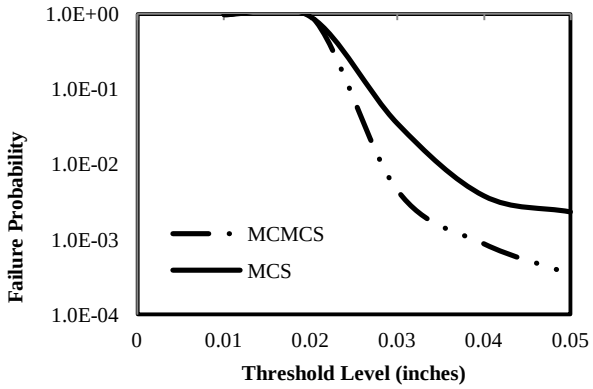

Fig. 8. Estimation for the probability of failure for different threshold levels σ_0 for case B (γ=1).

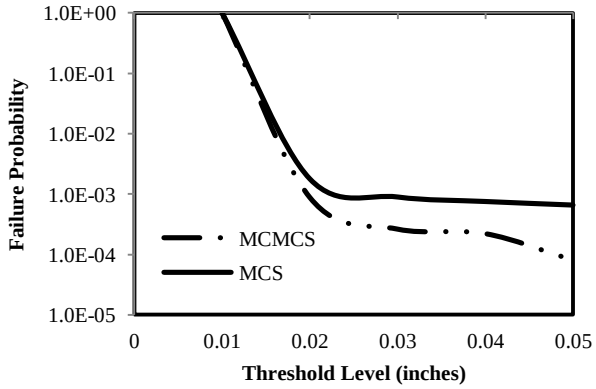

Fig. 9. Estimation for the probability of failure for different threshold levels σ_0 for case C (γ=1).

Figures demonstrate that for large failure probabilities, both of MCMCS and MCS methods have close responses, as an example, in case B, for threshold level $\sigma_0 = 0.01$, the probability of failure is 0.982 using the MCMCS method and 0.983 using the MCS method with equal number of samples, but with increasing the threshold level and decreasing the failure probability, MCMCS method provides smaller responses, as an example, in case B, for threshold level $\sigma_0 = 0.05$, the probability of failure is 3.43×10^{-4} using the MCMCS method and 2.33×10^{-3} using the MCS method. Therefore, the MCMCS method is an appropriate method for calculating the failure probability and the reliability index, for MDOF tendon controlled structures.

Figures 10, 11 and 12 present the cumulative probability distributions for the top floor RMS displacement response obtained via MCS method.

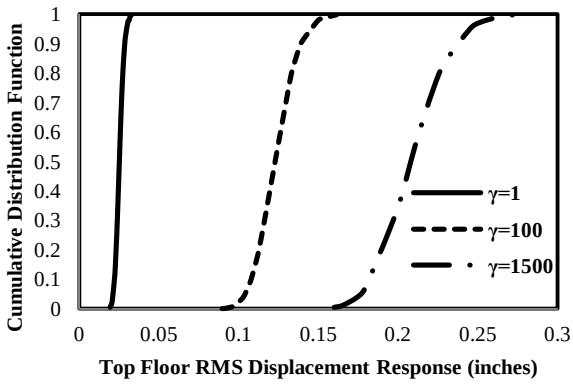

Fig. 10. Cumulative probability distribution functions of the top floor RMS displacement response (case A).

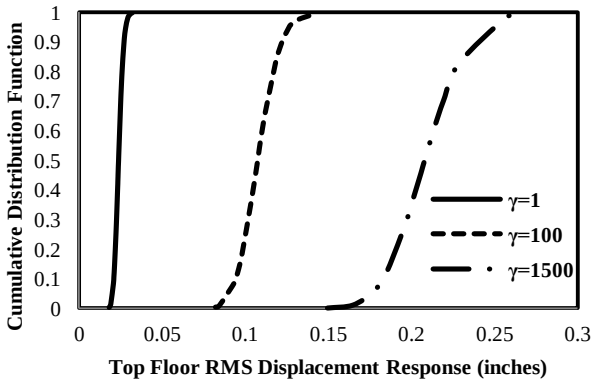

Fig. 11. Cumulative probability distribution functions of the top floor RMS displacement response (case B).

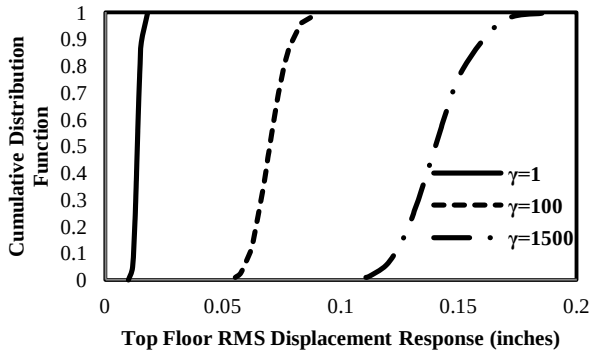

Fig. 12. Cumulative probability distribution functions of the top floor RMS displacement response (case C).

In all cases with increasing the control design parameter (γ), the effects of control forces decrease and the RMS displacement responses go to larger values. Fig. 13 shows that with use of smaller control design parameter, smaller failure probabilities obtain. Therefore with use of active control strategies, the failure probability decreases and consequently, the reliability index increases.

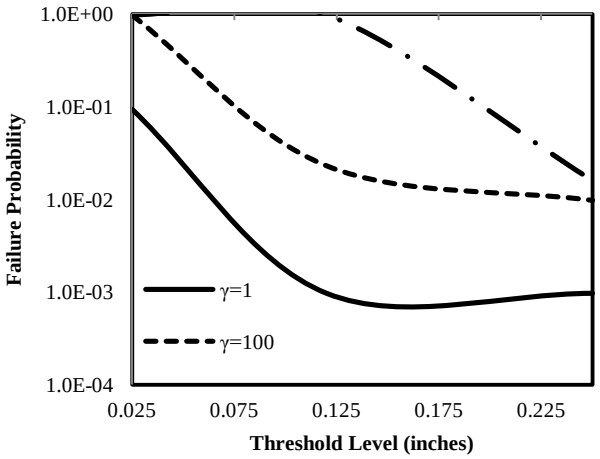

Fig. 13. Estimation for the probability of failure for different threshold levels σ_0 for different control design parameter γ.

Table 11 provides the nominal value of top floor RMS response for three cases of structure and Fig. 14 presents the cumulative probability distributions for the top floor RMS displacement response obtained via MCS method.

Table 11
Nominal value of top floor RMS response

	γ	x
case A	1	2.51E-02
	100	1.08E-01
	1500	2.08E-01
case B	1	2.38E-02
	100	1.08E-01
	1500	2.08E-01
case C	1	1.35E-02
	100	6.97E-02
	1500	1.40E-01

The results show that for multiple degree of freedom systems, placement of active tendons at first storey is insufficient. System can be more effective if active tendons are applied to all floors.

Active tendons at upper floors have a side effect. Tendons have reaction forces and these forces which are opposite to the direction of main control forces. But, in Case C, these reaction forces are supported by the ground so that the top floor RMS displacement response is smaller than Case B. The top floor RMS displacement response is the biggest in Case A as seen in Fig. 14.

Case C has more than one side effect. Tendons are very long and there are six actuators on the ground so that the application of this method is not practical. Also, the vertical components of control forces are bigger than other cases because of the increase of the tendon angles. These forces may also be harmful for the columns.

Tendons are useful for all ground acceleration records used for multiple degree of freedom systems. Consequently, the best case is B. Also, Case B is more practical to apply.

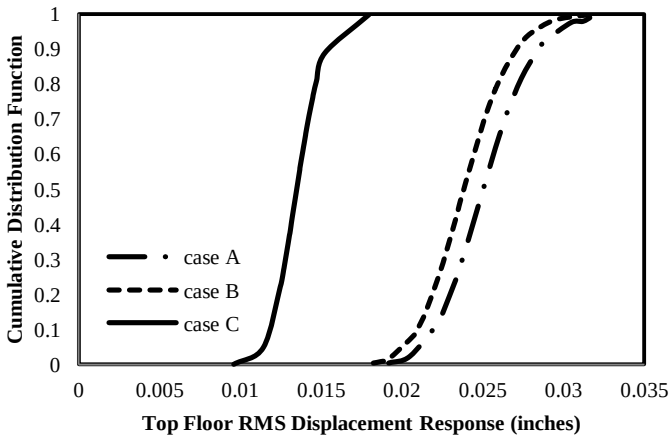

Fig. 14. Cumulative probability distribution functions of the top floor RMS displacement response for three cases.

7. Conclusion

Several illustrative examples in part I and part II verified the efficiency of the three reliability estimation methods. FORM provides a point estimate, subject to linearization errors, without confidence. Moreover, it requires the evaluation of the design point, which becomes difficult in high dimensions for non-linear limit state functions. Results show that only in limit state function with one design point, FORM has good result and in other cases cannot provide appropriate responses. The Monte Carlo simulation method has been widely used in the past because of its robustness and its ability to solve problems with complex failure regions. Its main disadvantage stems from its inefficiency when solving problems with large numbers of random variables and small probabilities (e.g.,$\mathrm{P_F} \leq 10^{-3}$), because the number of samples, and hence the number of system analyses required to achieve a given accuracy, is proportional to $1/\mathrm{P_F}$. Essentially, finding small probabilities requires information from rare samples corresponding to failure, and on average it would require many samples before a failure occurs, therefore MCS is not efficient method when the probability of failure is small. Subset simulation has a wide range of applicability. It performs well irrespectively of the geometry and the number of the failure domains. The advantages of this method include its accuracy, efficiency and its ability to handle structural systems with complex failure regions, large numbers of random variables, and small probabilities of failure.

Results obtained from three cases controlled system with active tendons show that by use of smaller control design parameter (γ), more weight is placed on the strain energy and smaller RMS displacement responses and smaller probability of failure obtain. Also although case C has smallest top floor RMS displacement response and smallest probability of failure, but tendons are very long and there are six actuators on the ground so that the application of this method is not practical, therefore case B is more practical to apply.

References

[1] Melchers RE. Structural reliability analysis and prediction. New York: John Wiley and Sons; 1999.

[2] Guan XL, Melchers RE. Effect of response surface parameter variation on structural reliability estimates. Struct Safety 2001;23:429–44.

[3] Fishman GS. Monte Carlo: concepts, algorithms, and applications. New York: Springer; 1996.

[4] Rubinstein RY. Simulation and the Monte-Carlo method. New York: Wiley; 1981.
[5] Pradlwarter HJ, Schuëller GI, Koutsourelakis PS, Charmpis DC. Application of line sampling simulation method to reliability benchmark problems. Struct
Safety 2007;29:208–21.
[6] Schuëller GI, Pradlwarter HJ, Koutsourelakis PS. A critical appraisal of reliability estimation procedures for high dimensions. Struct Safety 2004;19:463–74.
[7] Koutsourelakis PS, Pradlwarter HJ, Schuëller GI. Reliability of structures in high dimensions, part I: algorithms and applications. Struct Safety 2004;19:409–17.
[8] Au SK, Beck JL. Estimation of small failure probabilities in high dimensions by subset simulation. Probabilist Eng Mech 2001;16:263–77.
[9] Au SK. Probabilistic failure analysis by importance sampling Markov Chain simulation. J Eng Mech 2004;130:303–11.
[10] Metropolis N, Rosenbluth AW, Rosenbluth MN, Teller AH. Equations of states calculations by fast computing machines. J Chem Phys 1953; 21(6):1087-92.
[11] Miao F, Ghosn M. Modified subset simulation method for reliability analysis of structural systems. Struct Safety 2011; 33:251–260.
[12] Engelund S, Rachwitz R. A benchmark study on importance sampling techniques in structural reliability. Struct Safety 1993;12:255–76.
[13] Borri A, Speranzini E. Structural reliability analysis using a standard deterministic finite element code. Struct Safety 1997;19:361–82.
[14] Kiureghian AD, Lin HZ, Hwang SJ. Second-order reliability approximations. J Eng Mech Div, ASCE 1987;113:1208–25.
[15] Au SK, Beck JL. A new adaptive importance sampling scheme. Struct Safety 1999;21:135–58.
[16] Stochastic Finite Element Methods and Reliability, A State-of-the-Art Report, Report No. UCB/SEMM-2000/08, Department of Civil and Environmental Engineering, Univerisity of California, Berkeley, 2000.
[17] Chung LL, Reinhorn AM, Soong TT. Experiments on Active Control of Seismic Structures. J Eng Mech 1988;
114:241-25.
[18] Chung LL, Lin RC, Reinhorn AM, Soong TT. Experimental Study of Active Control for MDOF Seismic Structures. J Eng Mech 1989;115:1609-1627.
[19] Suhardjo J, Spencer Jr BF, Sain MK. Feedback-feedforward control of structures under seismic excitation. Struct Safety 1990;8:69-89.
[20] Soong TT, Grigoriu M. Random Vibration of Mechanical and Structural Systems. Prentice-Hall, Englewood
Cliffs, N.J., 1992.
[21] Nigdeli SM. Control of Structures with Active Tendons. M. H. Boduroğlu, thesis supervisor. İstanbul Technical University, Institute of science, M.Sc. thesis, 2007.
[22] Spencer Jr BF, Sain MK, Won CH, Kaspari DC, Sain PM. Reliability-based measures of structural control robustness. Struct Safety 1994;15:111-129.
[23] Sedarat H, Kosut R. Active Control in Structures. in 13th ASCE Engineering Mechanics Division Conference, Baltimore, 1999.